J. Am. Soc. Mass Spectrom. (2011) 22:1197–1203
DOI: 10.1007/s13361-011-0147-3

RESEARCH ARTICLE

Diagnostic NH and OH Vibrations for Oxazolone and Diketopiperazine Structures: b_2 from Protonated Triglycine

Da Wang, Kerim Gulyuz, Corey N. Stedwell, Nick C. Polfer

Department of Chemistry, University of Florida, Box 117200, Gainesville, FL 32611–7200, USA

Abstract

We present infrared multiple photon dissociation (IRMPD) spectra in the hydrogen stretching region of the simplest b fragment, b_2 from protonated triglycine, contrasted to that of protonated cyclo(Gly-Gly). Both spectra confirm the presence of intense, diagnostic vibrations linked to the site of proton attachment. Protonated cyclo(Gly-Gly) serves as a reference spectrum for the diketopiperazine structure, showing a diagnostic O-H^+ stretch of the protonated carbonyl group at 3585 cm^{-1}. Conversely, b_2 from protonated triglycine exhibits a strong band at 3345 cm^{-1}, associated with the N-H stretching mode of the protonated oxazolone ring structure. Other weaker N-H stretches can also be discerned, such as the amino NH_2 and amide NH bands. These results demonstrate the usefulness of the hydrogen stretching region, and hence benchtop optical parametric oscillator/amplifier (OPO/A) set-ups, in making structural assignments of product ions in collision-induced dissociation (CID) of peptides.

Key words: IRMPD spectroscopy, Oxazolone, Diketopiperazine, Glycine, Vibrations, Peptide fragmentation, Collision-induced dissociation, OPO

Introduction

Infrared multiple photon dissociation (IRMPD) spectroscopy [1–3] is one of the most useful tools in elucidating the chemistry of peptide dissociation in the gas phase by virtue of chemically diagnostic vibrations that can be identified [4]. One of the "textbook" examples of this approach involves verifying the oxazolone structure of "b" fragment ions [5, 6] formed from collision-induced dissociation (CID) of protonated peptides. A number of studies have shown that such structures exhibit diagnostic oxazolone C=O stretch bands that fall in the higher-frequency region of the mid-IR spectrum (i.e., 1780–1950 cm^{-1}) [7–14]. Nonetheless, in other cases head-to-tail cyclic "b" fragments were identified, so-called macrocycle structures, based on an absence of oxazolone-specific bands [15], and the presence of a proton bending mode at ~1440 cm^{-1} [8, 13, 14]. For the smallest b_2 fragments, such cyclic structures are known as diketopiperazine structures [16]. The majority of IRMPD spectroscopy studies on b_2 fragments have so far identified oxazolone structures [9, 10, 13, 14]; however, for instance for histidine-containing b_2, a mixture of oxazolone and diketopiperazine structures was confirmed [12].

All IRMPD spectroscopy studies described above have been carried out at the free electron laser (FEL) facilities FELIX in The Netherlands or CLIO in France [17, 18]. FELs are ideally suited to carry out IRMPD spectroscopy measurements, as their light output is intense (i.e., >MW), relatively broad (i.e., full-width half-maximum=1% central wavelength), and widely tunable (i.e., 50–2000 cm^{-1}). Moreover, the pulse structure of an FEL involves thousands

Electronic supplementary material The online version of this article (doi:10.1007/s13361-011-0147-3) contains supplementary material, which is available to authorized users.

Correspondence to: Nick Polfer; *e-mail:* polfer@chem.ufl.edu

Received: 25 February 2011
Revised: 3 April 2011
Accepted: 4 April 2011
Published online: 13 May 2011

of micropulses at a high repetition rate (i.e., GHz or 25 MHz, yielding 10–60 mJ per macropulse), which mirrors the mechanism of multiple photon absorption [19, 20].

Benchtop optical parametric oscillator/amplifier (OPO/A) set-ups generate radiation in the hydrogen stretching region (2200–4000 cm^{-1}) and have been employed in infrared photodissociation spectroscopy of van der Waals-tagged gas-phase complexes since the mid-1980s [21–26]. Only in the past decade, further developments of OPOs allowed IRMPD spectroscopy experiments on trapped ions in mass spectrometers [27]. Most of these photodissociation experiments have been carried out on relatively weakly-bound complexes, such as metal- and/or water-tagged complexes [28–36].

In contrast to FELs, the pulse structure of OPOs presents challenges to efficient IRMPD of trapped ions. Using a custom-built set-up in which the ions are photodissociated in a reduced-pressure (~10^{-5} mbar) quadrupole ion trap, we have recently shown that covalently-bound molecules, such as protonated tryptophan can be abundantly photodissociated using a benchtop continuous wave (cw) OPO [37], which produces narrowband radiation (i.e., <0.1 cm^{-1}).

Here, we apply this set-up to measure the IRMPD spectrum of a b_2 fragment, generated from protonated triglycine, in the hydrogen stretching region. The fragmentation chemistry for this ion has been studied extensively by others [38–41] and, hence, presents a suitable reference system. Moreover, in a previous mid-IR study using FELIX, it had been shown that this fragment ion adopts an oxazolone structure protonated on the oxazolone ring N [13]. It will be shown that a similar distinction between oxazolone and diketopiperazine structures is possible in the hydrogen stretching region based on diagnostic vibrations.

Experimental and Calculations

All experiments were performed using a tunable, continuous-wave (cw) optical parametric oscillator/amplifier (OPO/A) (LINOS Photonics OS4000, Munich, Germany) tethered to a custom-built mass spectrometer described in detail elsewhere [37, 42]. Briefly, this instrument is composed of a commercial electrospray ionization (ESI) source (Analytica, Branford, CT, USA) for generation of protonated peptides, a quadrupole mass filter (Ardara Technologies LP, Ardara, PA, USA) for mass selection of the precursor ion of interest, a reduced-pressure (~10^{-5} mbar) quadrupole ion trap (QIT) to irradiate the ions with focused laser irradiation, and a time-of-flight drift (TOF) tube (Jordan TOF Products, Grass Valley, CA, USA) for mass analysis of the remaining precursor and photodissociation products. The focused beam in the trap is equivalent to ~300 W/cm^2, following focusing of a ~25 mW cw idler beam to a beam waist<100 μm.

The peptide triglycine (Sigma Aldrich, St. Louis, MO, USA) was ionized in the protonated form by ESI. This peptide was subjected to collision-induced dissociation (CID) via "nozzle-skimmer" fragmentation in the ion source by adjusting the voltage drop between the exit voltage of the metalized glass capillary and the skimmer. The b_2 fragment generated from protonated triglycine, b_2-G3 (at *m/z* 115), was mass-selectively stored in the quadrupole ion trap for laser irradiation (2 or 3.5 s) with the tunable idler wavelength output of the benchtop OPO. The abundances of precursor *vs.* photofragment ions were obtained by integrating the TOF mass spectral peaks with an in-house LabView (National Instruments) software. The IRMPD yield, defined here as $\text{yield} = -\ln[1 - \Sigma(\text{photofragments})/\Sigma(\text{photofragments} + \text{precursor})]$, is then plotted as a function of laser frequency in cm^{-1} to obtain the IRMPD spectrum. Note, that the IRMPD yield was also normalized linearly with laser power. The IRMPD spectrum of protonated cyclo(Gly-Gly) (*m/z* 115) (Bachem, Torrance, CA), cyclo(Gly-Gly)H^+, was obtained in the same way as described above, without the need to generate a fragment ion in the ESI source. For example mass spectra for b_2-G3 and cyclo(Gly-Gly)H^+, see Figures S1 and S2 in the Supporting Information.

Three distinct chemical structures had to be considered in this study: oxazolone protonated on the oxazolone ring N (oxazolone ox-prot), oxazolone protonated on the N-terminus (oxazolone N-prot), and the diketopiperazine structure protonated on a carbonyl O (diketopiperazine O-prot). The computations for these structures had already been carried out in a previous study by Chen et al. [13] and, hence, the same geometries and spectra calculated at the B3LYP/6-31 g+(d,p) level of theory are employed here. The energies are reported on a relative scale as zero-point energy (ZPE)-corrected energies. The harmonic spectra were scaled by a constant scaling factor of 0.9648, as recommended by Merrick et al. for this level of theory [43]. The stick spectra were broadened by a Gaussian function (full-width at half-maximum=20 cm^{-1}) to allow a more facile comparison to experiment. Finally, the convoluted spectra were normalized to integral band intensities in km mol^{-1} for more convenient comparison of vibrational intensities.

Results and Discussion

IRMPD Spectroscopy Results

In the previous structural characterization of b_2-G3 in the mid-IR range, the IRMPD spectrum of cyclo(Gly-Gly)H^+ served as a control experiment for the diketopiperazine structure [13]. The IRMPD spectra of b_2-G3 and cyclo(Gly-Gly)H^+ in the hydrogen stretching range, 3250–3700 cm^{-1}, are contrasted in Figure 1. Each spectrum displays an intense, characteristic band, demonstrating that both isomeric structures can in fact be easily distinguished. For b_2-G3, the band at 3345 cm^{-1} corresponds to the N-H stretching mode of the protonated oxazolone ring structure, whereas for cyclo(Gly-Gly)H^+, the band at 3585 cm^{-1} is assigned to the proton stretching

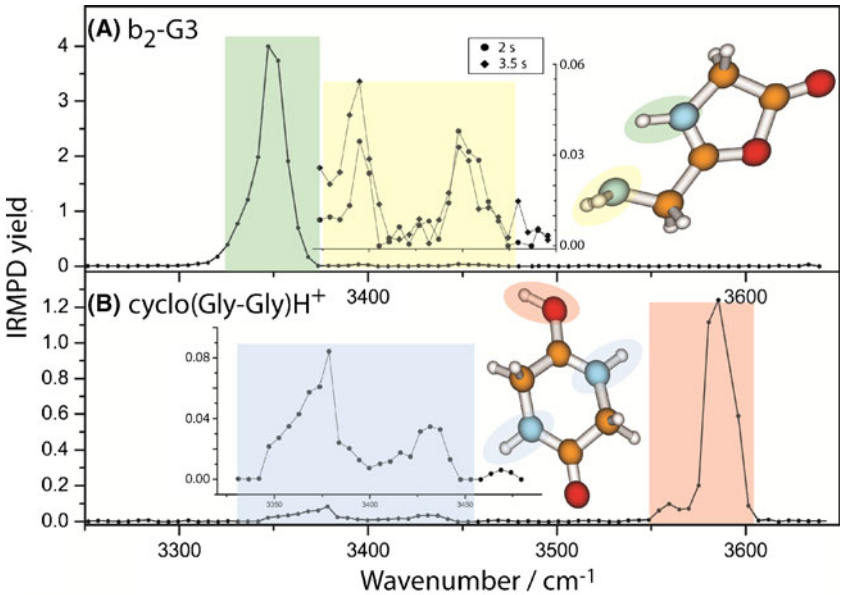

Figure 1. IRMPD spectra of (**A**) b_2 from protonated triglycine, and (**B**) protonated cyclo(Gly-Gly). The insets show blow-ups of weaker bands in the NH stretching region. The diagnostic modes are indicated by color-coding

mode of the diketopiperazine structure protonated on a carbonyl O. Other weaker features, corresponding to other NH stretching modes, can be discerned in both spectra (see insets). All structurally diagnostic modes are indicated by color-coding, and are summarized in Table 1. These will be discussed in more detail below (see Comparison to Theory section). As a general observation, one can see that photofragmentation of b_2-G3 was more facile than for cyclo(Gly-Gly)H^+ under identical experimental conditions. The maximum IRMPD yield for b_2-G3 was 4 (corresponding to 98% depletion of the precursor ion), compared to a maximum value of 1.2 for cyclo(Gly-Gly)H^+ (corresponding to 70% depletion of the precursor ion). The transition state for b_2 (*m/z* 115) → a_2 (*m/z* 87) had been calculated by Paizs et al. to be a relatively low 26.2 kcal mol^{-1} for a one-step elimination process of CO [44]. This corresponds to >9160 cm^{-1}, and hence an absorption of at least three photons in this frequency region. There were also some differences in the photofragment products: irradiation of b_2-G3 resulted in appearance of an abundant photofragment at *m/z* 87 (i.e., $\mathbf{a_2}$) and some at *m/z* 59; irradiation of cyclo(Gly-Gly)H^+ gave rise to photodissociation product at *m/z* 87, as well as some at *m/z* 70 (a_2-NH_3) (see Figures S1 and S2).

Comparison to Theory

A comparison of the experimental spectrum for b_2-G3 to the computed spectra for oxazolone ox-prot and oxazolone N-prot is shown in Figure 2. It is concluded that the predicted oxazolone ox-prot N-H stretch matches well with the strong band at 3345 cm^{-1}, and the weaker features at 3395 and 3450 cm^{-1}, assigned to the symmetric and antisymmetric NH_2 modes. Conversely, the predicted intense symmetric NH_3^+ stretching band for oxazolone N-prot at ~2900 cm^{-1} is not confirmed. Note that the higher-frequency NH_3^+ modes would be more difficult to exclude, as they overlap with oxazolone ox-prot NH stretches. Another indication for the exclusive presence of oxazolone ox-prot is the near-total photodepletion of the parent ion (~98%) at the diagnostic band for this structure (i.e., 3345 cm^{-1}). These results confirm the previous

Table 1. Summary of Centroid Band Positions and Spectral Assignments for IRMPD Spectra in Figure 1. The Unscaled Frequencies for *Oxazolone Ox-prot* (Figure 2) and *Diketopiperazine O-prot* (Figure 3), Calculated at B3LYP/6-31 g+(d,p), As Well as Ideal Scaling Factors are Indicated

Band position/cm^{-1}	Assignment	Unscaled frequencies at B3LYP/6-31 g+(d,p)/cm^{-1} (ideal scaling factor)
b_2-G3		
3345	Protonated oxazolone N-H stretch	3485 (0.960)
3395	Symmetric NH_2 stretch	3533 (0.961)
3450	Antisymmetric NH_2 stretch	3612 (0.955)
cyclo(Gly-Gly)H^+		
3370	Amide N-H (closest to O-H^+)	3509 (0.960)
3430	Amide N-H (furthest away from O-H^+)	3583 (0.957)
3585	Protonated carbonyl O-H^+	3704 (0.968)

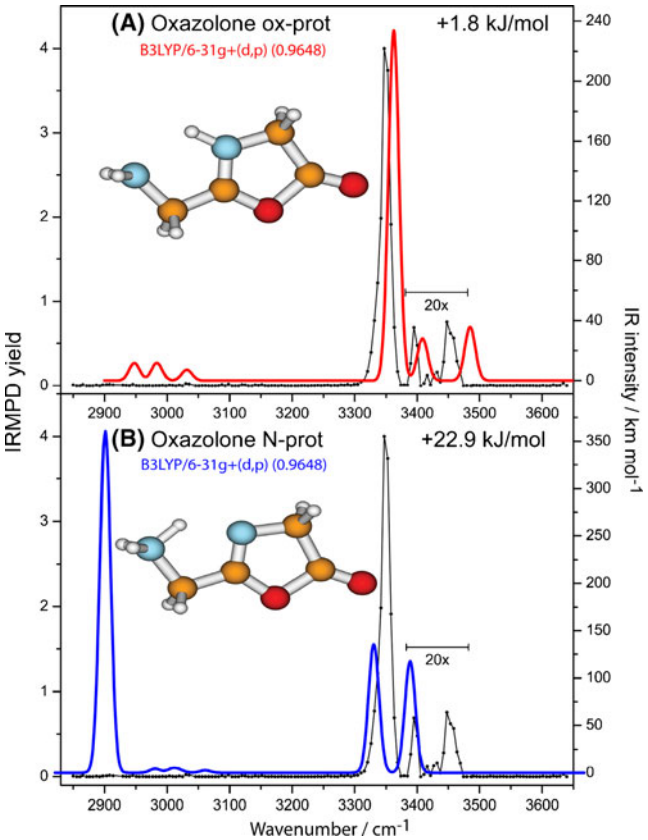

Figure 2. IRMPD spectrum of b_2-G3 compared to the computed spectra of the lowest-energy conformers for (**A**) oxazolone ox-prot (in red) and (**B**) oxazolone N-prot (in blue). The intensities of the spectral region covering the NH_2 bands is expanded 20× to allow an easier comparison to the computed spectra

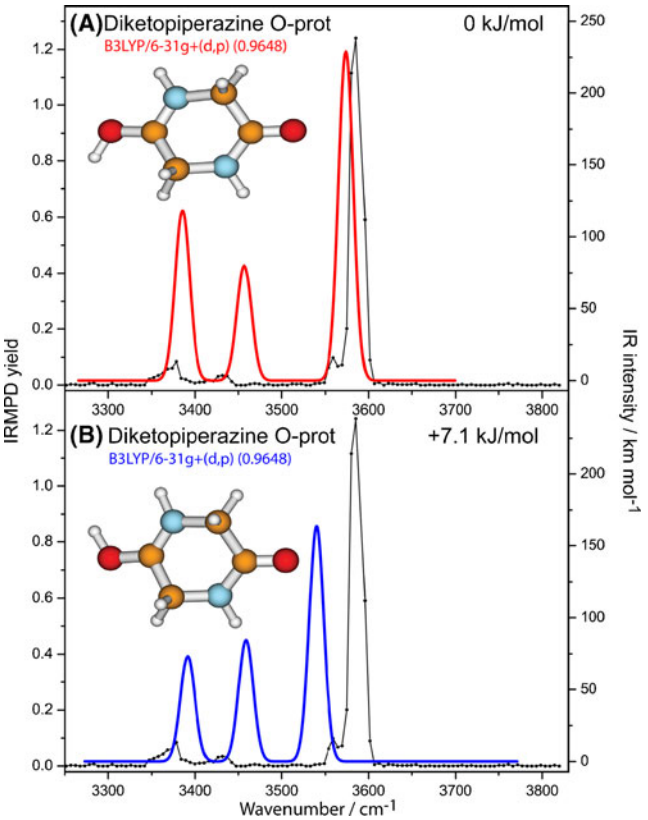

Figure 3. IRMPD spectrum of cyclo(Gly-Gly)H^+ compared with the lowest-energy conformers for diketopiperazine O-prot (A+B)

mid-IR results, where exclusively oxazolone ox-prot structures were proposed to be present [13]. In addition, the computed thermochemistries also suggest an absence of oxazolone N-prot at room temperature.

In Figure 3, the experimental IRMPD spectrum for cyclo(Gly-Gly)H^+ is compared with the computed spectra of the lowest-energy diketopiperazine O-prot structures. The intense O-H^+ stretching mode at 3585 cm^{-1} and the amide N-H stretches at 3370 and 3430 cm^{-1} are compatible with the lowest-energy (i.e., 0 kJ mol^{-1}) geometry. The weaker feature at 3560 cm^{-1}, red-shifted with respect to the main 3585 cm^{-1} band, is consistently reproduced. A tentative assignment is made to the O-H^+ stretch of the higher-energy (+7.1 kJ mol^{-1}) diketopiperazine O-prot, where the proton is turned towards the amide NH group, as opposed to the CH_2 group. This energy gap should be thermally accessible at room temperature (within the accuracy of the calculation), thus potentially rationalizing a small population of the higher-energy conformation.

Experimental Band Intensities

As a general observation, the band intensities of the weaker NH modes (i.e., NH_2 and amide NH) are found to be much weaker experimentally than predicted by theory (compared with the stronger modes). Similar observations had been made before for experimental studies involving this OPO set-up [36, 37, 42]. Since IRMPD necessitates the absorption of multiple photons, the IRMPD yield is subject to non-linear processes. Systematic studies on this set-up had shown that the IRMPD yield was reasonably linear as a function of OPO power and irradiation time, but only within particular kinetic windows [42]. Below a certain OPO power (~8 mW), no photodissociation was observed. For weaker modes, the corresponding power threshold is higher. The weak CH stretching modes, predicted around 3000 cm^{-1} in Figure 2, require a higher power threshold than is achievable experimentally, and are thus not observed. Given these differences in OPO power thresholds for different vibrations, the IRMPD experiments often require multiple irradiation lengths to visualize both stronger and weaker modes in the same spectrum.

General Considerations for Diagnostic NH and OH Band Positions

The use of a suitable scaling factor is a caveat in the interpretation of IRMPD spectra. In Table 1, the ideal scaling factors for each vibration are shown, based on matching of the unscaled calculated frequencies to experimentally derived IRMPD centroid band positions. It can be

seen that the scaling factor of 0.9648 is more suitable for the O-H^+ stretch than for the various NH stretches. As a result of this scaling factor, the NH stretches are predicted at higher frequencies than where they are observed. Some studies have employed a single scaling factor for all vibrations (e.g., 0.952 by Rizzo and coworkers [45], and 0.96 by Mons and coworkers [46]), depending on the level of theory that was chosen. Others have employed variable scaling factors for NH and OH vibrations (e.g., 0.956 for NH and 0.976 for OH by Snoek and coworkers [47], and 0.959 for NH and 0.976 for OH by Lisy and coworkers [48]). The use of different scaling factors for NH and OH vibrations is often warranted, due to differences in the anharmonicities for OH and NH modes, which harmonic calculations do not account for. In some cases, the use of different scaling factors is required, such as in the case of protonated tryptophan, where both the indole NH and carboxylic acid OH stretch were theoretically predicted at the same frequency, but were experimentally resolved from one another [37]. For the diagnostic modes reported here, the NH stretching modes would benefit from a scaling factor of 0.959. However, the O-H^+ stretching mode would be ill-matched by a scaling factor of 0.976. More experimental studies on other b fragments will be required to establish a generally suitable scaling factor for the O-H^+ stretch.

Typically, OH stretches are measured at higher frequencies than NH stretches, which is related to the higher O–H bond strength. Nonetheless, hydrogen bonding can result in significant red-shifting of bands, and hence the diagnostic band positions reported here for glycine-based b_2 are likely to shift in other b fragments. In fact, for the macrocyclic (i.e., cyclic peptide) O-H^+ stretch frequency, large frequency shifts are expected as a function of the b fragment size. If the proton is located between two chemical binding sites, the frequency of a proton-bound mode can vary from 3700 cm^{-1} (for ligands with large differences in proton affinity) all the way down to <1000 cm^{-1} (for ligands with equivalent proton affinities) [49]. The extremely low vibrational frequencies for "shared" protons are due to a flat anharmonic potential, which also manifests itself in broad vibrational features, as shown in IRMPD studies on proton-bound dimers [50–52]. In terms of b fragments, the IR frequency of a diagnostic O-H^+ stretch, when the proton is located on a backbone carbonyl O, is likely to shift to lower frequencies for larger b fragments, as more carbonyl binding sites are available. In fact, the broad band observed by Chen et al. between 2500 and 2700 cm^{-1} for the glycine-based b_5-type fragment is consistent with some sharing of the proton between two carbonyl oxygens in a macrocycle structure [13].

Conclusions

The IRMPD spectrum for b_2 (generated from protonated triglycine) has been compared with a reference spectrum for protonated cyclo(Gly-Gly) to demonstrate that the hydrogen stretching region is well suited to the structural distinction of oxazolone and diketopiperazine structures. The structurally diagnostic modes are related to proton-bound modes of the protonated oxazolone ring N-H stretch (at 3345 cm^{-1}) and the diketopiperazine protonated carbonyl O-H^+ stretch (at 3585 cm^{-1}).

In contrast to previous IRMPD studies recorded at free electron laser facilities, these spectra were acquired using a benchtop optical parametric oscillator in combination with a reduced-pressure quadrupole ion trap. The results show that covalently-bound product ions made from collision-induced dissociation (CID) can now be routinely and efficiently photodissociated using a relatively weak continuous-wave OPO. Given the many sequence variations that can be considered in peptides, more systematic studies are required to obtain insights into the overall trends in fragmentation chemistry in tandem mass spectrometry. Due to the limitation of beamtime at FEL facilities, it is expected that approaches involving OPOs will be essential to address this challenge, in order to make IRMPD spectroscopy available to the wider mass spectrometry community.

Acknowledgments

This material is based upon work supported by the National Science Foundation under CHE-0845450. N.C. P. thanks the University of Florida for generous start-up funds. Professor John Eyler is thanked for providing access to his OPO, which was funded from an In-House Research Program (IHRP) grant from the National High Magnetic Field Laboratory (NHMFL). The authors' collaborators from Ardara Technologies and, particularly, Randall E. Pedder, Christopher Taormina, and Dodge Baluya are acknowledged for their help in designing and setting up the custom-built mass spectrometer described here. Damon T. Allen is acknowledged for writing the LabView software employed in the mass spectral analysis. Finally, the authors thank their colleagues in the mechanical and electronic workshops in the department of chemistry for all their help and, in particular, Todd Prox, Brian Smith, and Steven Miles.

References

1. Eyler, J.R.: Infrared multiple photon dissociation spectroscopy of ions in Penning traps. *Mass Spectrom. Rev.* **28**, 448–467 (2009)
2. Fridgen, T.D.: Infrared consequence spectroscopy of protonated and metal ion cationized complexes. *Mass Spectrom. Rev.* **28**, 586–607 (2009)
3. Polfer, N.C.: Infrared multiple photon dissociation spectroscopy of trapped ions. *Chem. Soc. Rev.* **40**, 2211–2221 (2011)
4. Polfer, N.C., Oomens, J.: Reaction products in mass spectrometry elucidated with infrared spectroscopy. *Phys. Chem. Chem. Phys.* **9**, 3804–3817 (2007)
5. Yalcin, T., Khouw, C., Csizmadia, I.G., Peterson, M.R., Harrison, A.G.: Why are b ions stable species in peptide spectra? *J. Am. Soc. Mass Spectrom.* **6**, 1165–1174 (1995)
6. Yalcin, T., Csizmadia, I.G., Peterson, M.B., Harrison, A.G.: The structure and fragmentation of b_n ($n \geq 3$) ions in peptide spectra. *J. Am. Soc. Mass Spectrom.* **7**, 233–242 (1996)
7. Polfer, N.C., Oomens, J., Suhai, S., Paizs, B.: Spectroscopic and theoretical evidence for oxazolone ring formation in collision-induced dissociation of peptides. *J. Am. Chem. Soc.* **127**, 17154–17155 (2005)
8. Polfer, N.C., Oomens, J., Suhai, S., Paizs, B.: Infrared spectroscopy and theoretical studies on gas-phase protonated leu-enkephalin and its

fragments: direct evidence for the mobile proton. *J. Am. Chem. Soc.* **129**, 5887–5897 (2007)
9. Yoon, S., Chamot-Rooke, J., Perkins, B., Hilderbrand, A.E., Poutsma, J., Wysocki, V.H.: IRMPD spectroscopy shows that AGG forms an oxazolone b ion. *J. Am. Chem. Soc.* **130**, 17644–17645 (2008)
10. Oomens, J., Young, S., Molesworth, S., van Stipdonk, M.J.: Spectroscopic evidence for an oxazolone structure of the b_2 fragment ion from protonated tri-alanine. *J. Am. Soc. Mass Spectrom.* **20**, 334–339 (2009)
11. Bythell, B., Erlekam, U., Paizs, B., Maitre, P.: Infrared spectroscopy of fragments from doubly protonated tryptic peptides. *Chem. Phys. Chem.* **10**, 883–885 (2009)
12. Perkins, B., Chamot-Rooke, J., Yoon, S., Gucinski, A., Somogyi, A., Wysocki, V.H.: Evidence of diketopiperazine and oxazolone structures for HA b_2^+ ion. *J. Am. Chem. Soc.* **131**, 17528–17529 (2009)
13. Chen, X., Yu, L., Steill, J.D., Oomens, J., Polfer, N.C.: Effect of peptide fragment size on the propensity of cyclization in collision-induced dissociation: oligoglycine b_2-b_8. *J. Am. Chem. Soc.* **131**, 18272–18282 (2009)
14. Chen, X., Steill, J.D., Oomens, J., Polfer, N.C.: Oxazolone versus macrocycle structures for Leu-enkephalin b2-b4: Insights from infrared multiple-photon dissociation spectroscopy and gas-phase hydrogen/deuterium exchange. *J. Am. Soc. Mass Spectrom.* **21**, 1313–1321 (2010)
15. Erlekam, U., Bythell, B., Scuderi, D., Van Stipdonk, M.J., Paizs, B., Maitre, P.: Infrared spectroscopy of fragments of protonated peptides: direct evidence for macrocyclic structures of b5 ions. *J. Am. Chem. Soc.* **131**, 11503–11508 (2009)
16. Cordero, M., Houser, J., Wesdemiotis, C.: The neutral products formed during backbone fragmentations of protonated peptides in tandem mass spectrometry. *Anal. Chem.* **65**, 1594–1601 (1993)
17. Oepts, D., van der Meer, A.F.G., van Amersfoort, P.W.: The free-electron-laser user facility FELIX. *Infrared Phys. Technol.* **36**, 297–308 (1995)
18. Lemaire, J., Boissel, P., Heninger, M., Mauclaire, G., Bellec, G., Mestdagh, H., Simon, A., Caer, S.L., Ortega, J.-M., Glotin, F., Maitre, P.: Gas phase infrared spectroscopy of selectively prepared ions. *Phys. Rev. Lett.* **89**, 273002 (2002)
19. Bagratashvili, V.N., Letokov, V.S., Makarov, A.A., Ryabov, E.A.: Multiple photon infrared laser photophysics and photochemistry. Harwood Acaemic, Chur (1985)
20. Oomens, J., Sartakov, B., Meijer, G., von Helden, G.: Gas-phase infrared multiple photon dissociation spectroscopy of mass-selected molecular ions. *Int. J. Mass Spectrom.* **254**, 1–19 (2006)
21. Okumura, M., Yeh, L., Lee, Y.T.: The vibrational predissociation spectroscopy of hydrogen cluster ions. *J. Chem. Phys.* **83**, 3705–3706 (1985)
22. Okumura, M., Yeh, L., Myers, J.D., Lee, Y.T.: Infrared spectra of the cluster ions $H_7O_3^+.H_2$ and $H_9O_4^+.H_2$. *J. Chem. Phys.* **85**, 2328–2329 (1986)
23. Cabarcos, O.M., Weinheimer, C.J., Lisy, J.M.: Size selectivity by cation-p interactions: solvation of K^+ and Na^+ by benzene and water. *J. Chem. Phys.* **110**, 8429–8435 (1999)
24. Headrick, J.M., Diken, E.G., Walters, R.S., Hammer, N.I., Christie, R. A., Cui, J., Myshakin, E.M., Duncan, M.A., Johnson, M.A., Jordan, K. D.: Spectral signatures of hydrated proton vibrations in water clusters. *Science* **308**, 1765–1769 (2005)
25. Pillai, E.D., Jaeger, T.D., Duncan, M.A.: IR spectroscopy of $Nb^+(N_2)_n$ complexes: coordination, structures, and spin states. *J. Am. Chem. Soc.* **129**, 2297–2307 (2007)
26. Elliott, B.M., Relph, R.A., Roscioli, J.R., Bopp, J.C., Gardenier, G.H., Guasco, T.L., Johnson, M.A.: Isolating the spectra of cluster ion isomers using Ar-"tag"-mediated IR-IR double resonance within the vibrational manifolds: application to $NO_2^-.H_2O$. *J. Chem. Phys.* **129**, 094303 (2008)
27. Oh, H., Breuker, K., Sze, S.K., Ge, Y., Carpenter, B.K., McLafferty, F.W.: Secondary and tertiary structures of gaseous protein ions characterized by electron capture dissociation mass spectrometry and photofragment spectroscopy. *Proc. Natl. Acad. Sci. U. S. A.* **99**, 15863–15868 (2002)
28. Oh, H., Lin, C., Hwang, H.Y., Zhai, H., Breuker, K., Zabrouskov, V., Carpenter, B.K., McLafferty, F.W.: Infrared photodissociation spectroscopy of electrosprayed ions in a Fourier transform mass spectrometer. *J. Am. Chem. Soc.* **127**, 4076–4083 (2005)
29. Kamariotis, A., Boyarkin, O.V., Mercier, S.R., Beck, R.D., Bush, M.F., Williams, E.R., Rizzo, T.R.: Infrared spectroscopy of hydrated amino acids in the gas phase: protonated and lithiated valine. *J. Am. Chem. Soc.* **128**, 905–916 (2006)
30. Bush, M.F., O'Brien, J.T., Prell, J.S., Saykally, R.J., Williams, E.R.: Infrared spectroscopy of cationized arginine in the gas phase: direct evidence for the transition from nonzwitterionic to zwitterionic structure. *J. Am. Chem. Soc.* **129**, 1612–1622 (2007)
31. Miller, D., Lisy, J.M.: Modeling competitive interactions in proteins: vibrational spectroscopy of $M^+(n\text{-methylacetamide})_1(H_2O)_{n\,=\,0-3}$, M= Na and K, in the 3 mm region. *J. Phys. Chem. A* **111**, 12409–12416 (2007)
32. Rajabi, K., Fridgen, T.D.: Structures of aliphatic amino acid proton-bound dimers by infrared multiple photon dissociation spectroscopy in the 700–2000 cm^{-1} region. *J. Phys. Chem. A* **112**, 23–30 (2008)
33. Cagmat, E., Szczepanski, J., Pearson, W., Powell, D.H., Eyler, J.R., Polfer, N.: Vibrational signatures of metal-chelated monosaccharide epimers: gas-phase infrared spectroscopy of Rb^+-tagged glucuronic and iduronic acid. *Phys. Chem. Chem. Phys.* **12**, 3474–3479 (2010)
34. Prell, J.S., Chang, T.M., O'Brien, J.T., Williams, E.R.: Hydration isomers of protonated phenylalanine and derivatives: relative stabilities from infrared photodissociation. *J. Am. Chem. Soc.* **132**, 7811–7819 (2010)
35. Rajabi, K., Gillis, E.A.L., Fridgen, T.D.: Structures of alkali metal ion-adenine complexes and hydrated complexes by IRMPD spectroscopy and electronic structure calculations. *J. Phys. Chem. A* **114**, 3449–3456 (2010)
36. Mino Jr., W.K., Szczepanski, J., Pearson, W., Powell, D.H., Dunbar, R.C., Eyler, J.R., Polfer, N.: Vibrational signatures of zwitterionic and charge-solvated structures for alkaline earth-tryptophan dimer complexes in the gas phase. *Int. J. Mass Spectrom.* **297**, 131–138 (2010)
37. Mino Jr., W.K., Gulyuz, K., Wang, D., Stedwell, C., Polfer, N.C.: Gas-phase structure and dissociation chemistry of protonated tryptophan elucidated by infrared multiple-photon dissociation spectroscopy. *J. Phys. Chem. Lett.* **2**, 299–304 (2011)
38. Morgan, D., Bursey, M.: A linear free-energy correlation in the low-energy tandem mass-spectra of protonated tripeptides Gly-Gly-Xxx. *Org. Mass Spectrom.* **29**, 354–359 (1994)
39. Paizs, B., Lendvay, G., Vekey, K., Suhai, S.: Formation of b(2)(+) ions from protonated peptides: an ab initio study. *Rapid Commun. Mass Spectrom.* **13**, 525–533 (1999)
40. Paizs, B., Suhai, S.: Combined quantum chemical and and RRKM modeling of the main fragmentation pathways of protonated GGG. Cis-trans isomerization around protonated amide bonds. *Rapid Commun. Mass Spectrom.* **15**, 2307–2323 (2001)
41. Paizs, B., Suhai, S.: Combined quantum chemical and RRKM modeling of the main fragmentation pathways of protonated GGG. II. Formation of b2, y1, and y2 ions. *Rapid Commun. Mass Spectrom.* **16**, 375–389 (2002)
42. Gulyuz, K., Stedwell, C., Wang, D., Polfer, N.C.: Hybrid quadrupole mass filter/quadrupole ion trap/time-of-flight-mass spectrometer for infrared multiple photon dissociation spectroscopy of mass-selected ions. *Rev. Sci. Instrum.* **82**, doi:10.1063/1.3585982 (2011)
43. Merrick, J.P., Moran, D., Radom, L.: An evaluation of harmonic vibrational frequency scale factors. *J. Phys. Chem. A* **111**, 11683–11700 (2007)
44. Paizs, B., Szlavik, Z., Lendvay, G., Vekey, K., Suhai, S.: Formation of a(2)(+) ions of protonated peptides: an ab initio study. *Rapid Commun. Mass Spectrom.* **14**, 746–755 (2000)
45. Stearns, J.A., Boyarkin, O.V., Rizzo, T.R.: Spectroscopic signatures of gas-phase helices: Ac-Phe-$(Ala)_5$-Lys-H^+ and Ac-Phe-$(Ala)_{10}$-Lys-H^+. *J. Am. Chem. Soc.* **129**, 13820–13821 (2007)
46. Brenner, V., Piuzzi, F., Dimicoli, I., Tardivel, B., Mons, M.: Chirality-controlled formation of b-turn secondary structures in short peptide chains: gas-phase experiment versus quantum chemistry. *Angew. Chem. Int. Ed Engl.* **46**, 2463–2466 (2007)
47. Vaden, T.D., de Boer, T., MacLoed, N., Marzluff, E., Simons, J.P., Snoek, L.C.: Infrared spectroscopy and structure of photochemically protonated biomolecules in the gas phase: a noradrenaline analogue, lysine, and alanyl alanine. *Phys. Chem. Chem. Phys.* **9**, 2549–2555 (2007)
48. Nicely, A.L., Miller, D.J., Lisy, J.M.: Charge and temperature dependence of biomolecule conformations: K^+tryptamine$(H_2O)_{n=0-1}Ar_{m\,=\,0-1}$ cluster ions. *J. Am. Chem. Soc.* **131**, 6314–6315 (2009)
49. Roscioli, J.R., McCunn, L.R., Johnson, M.A.: Quantum structure of the intermolecular proton bond. *Science* **316**, 249–254 (2007)

50. Asmis, K.R., Pivonka, N.L., Santambrogio, G., Brummer, M., Kaposta, C., Neumark, D.M., Woste, L.: Gas-phase infrared spectrum of the protonated water dimer. *Science* **299**, 1375–1377 (2003)
51. Moore, D.T., Oomens, J., van der Meer, A.F.G., von Helden, G., Meijer, G., Valle, J.J., Marshall, A.G., Eyler, J.R.: Probing vibrations of shared, OH^+O-bound protons in the gas phase. *Chem. Phys. Chem.* **5**, 740–743 (2004)
52. Fridgen, T.D., MacAleese, L., Maitre, P., McMahon, T.B., Boissel, P., Lemaire, J.: Infrared spectra of homogeneous and heterogeneous proton-bound dimers in the gas phase. *Phys. Chem. Chem. Phys.* **7**, 2747–2755 (2005)